Received: 22 July 2018 | Revised: 5 November 2018 | Accepted: 11 November 2018
DOI: 10.1002/ardp.201800219

FULL PAPER

DPhG ARCH PHARM
Archiv der Pharmazie

Liposomes actively recognizing the glucose transporter $GLUT_1$ and integrin $\alpha_v\beta_3$ for dual-targeting of glioma

Qiuyi Fu | Yi Zhao | Zhongzhen Yang | Qiming Yue | Wenjiao Xiao | Yang Chen | Yang Yang | Li Guo | Yong Wu

Key Laboratory of Drug Targeting and Drug Delivery System of Education Ministry, Department of Medicinal Chemistry, West China School of Pharmacy, Sichuan University, Chengdu, P. R. China

Correspondence
Prof. Li Guo and Dr. Yong Wu, Key Laboratory of Drug Targeting and Drug Delivery System of Education Ministry, Department of Medicinal Chemistry, West China School of Pharmacy, Sichuan University, Chengdu 610041, P. R. China.
Email: guoli@scu.edu.cn (L.G.), wyong@scu.edu.cn (Y.W.)

Funding information
Sichuan Science and Technology Program, Grant number: 2018JY0537; National Natural Science Foundation of China, Grant numbers: 21472130, 81573286, 81773577; the Fundamental Research Funds for the Central Universities, Grant number: 2012017yjsy211

Abstract

The treatment of glioma is a great challenge because of the existence of the blood–brain barrier (BBB). In order to develop an efficient glioma-targeting drug delivery system to greatly improve the brain permeability of anti-cancer drugs and target glioma, a novel glioma-targeted glucose-RGD (Glu-RGD) derivative was designed and synthesized as ligand for preparing liposomes to effectively deliver paclitaxel (PTX) to cross the BBB and target glioma. The liposomes were prepared and characterized for particle size, zeta potential, encapsulation efficiency, release profile, stability, hemolysis, and cell cytotoxicity. Also, the Glu-RGD modified liposomes showed superior targeting ability in *in vitro* and *in vivo* evaluation as compared to naked PTX, non-coated, singly modified liposomes and liposomes co-modified by physical blending. The relative uptake efficiency and concentration efficiency were enhanced by 4.41- and 4.72-fold compared to that of naked PTX, respectively. What is more, the Glu-RGD modified liposomes also displayed the maximum accumulation of DiD-loaded liposomes at tumor sites compared to the other groups in *in vivo* imaging. All the results *in vitro* and *in vivo* suggested that Glu-RGD-Lip would be a potential delivery system for PTX to treat integrin $\alpha_v\beta_3$-overexpressing tumor-bearing mice.

KEYWORDS
drug delivery, dual-targeting, glucose, liposomes, RGD peptide

1 | INTRODUCTION

Over the past few decades, with the rapid development of medical science, many diseases are gradually being overcome. But the central nervous system (CNS) diseases, such as brain tumor, have become one of the most dangerous threats to human health, due to dramatic increase of brain diseases and their lower recovery.[1–3] So, the treatment for brain tumor has become a pressing problem that needs to be solved. However, the poor brain permeability of anti-cancer drugs (including paclitaxel) limits their penetration across blood–brain barrier (BBB), which is formed by tightly connected endothelial cells of brain capillaries with the surrounding astrocytes and pericytes,[4] resulting in a poor effect in the brain. Although increasing the dose of drugs in treatments may increase the vascular-corrected brain concentration, it could cause stronger side effects and severer toxicity. Therefore, there is a huge amount of demand of, not only for paclitaxel (PTX) but in general, strategies that can effectively deliver drugs, including PTX, into the brain for the treatment of brain tumor.[5,6]

The dual-targeting drug delivery system was raised by several groups in 2009. With the development of targeting delivery system, the strategies for dual-targeting brain tumor were divided into three types.[7] The first type was to target two types of cells in brain tumor

with different ligands. Gao et al.[8] used IL-13p and RGD peptide to target glioma and neovasculature, respectively. The second type was one ligand with two different targeting warheads. Liu's group utilized R8-RGD to target BBB and glioma.[9] The third type was to target BBB and glioma with different ligands. Gao and his co-workers used transferrin to transport across the BBB and glucose analog to target glioma, which showed superior treatment effect for glioma.[10] Thus, an ideal dual-targeting drug delivery system should effectively transport across the BBB and target brain tumor.[11] In this paper, we will explore the possibility to develop a glioma-targeting liposomes drug delivery system which uses glucose and RGD peptide as the mediator to improve the delivery of drugs into brain tumor tissue.

Because of the high transport affinity between the transporter and substance, carrier-mediated transporter (CMT) system seems to be one of the most promising methods to facilitate the delivery of drugs into brain, among which $GLUT_1$ expressed on the surface of brain capillary endothelial cells is considered as one of the most efficient transport systems that can transport glucose across the BBB into brain effectively.[12] It is well known that the large and uninterrupted energy demand of the brain is provided almost exclusively by glucose, which is transported through the BBB by $GLUT_1$. It is estimated that the transport value of $GLUT_1$ is 15–3000 fold more than other transporters. Liposomes modified by glucose have been proposed as a strategy to improve their brain uptake. Moreover, it has been widely reported that C-6 position glycosylation is an effective way to heighten the accumulation of drugs in brain.[12,13] Our previous studies have also demonstrated that the glucose-modified liposomes could be delivered into brain specifically and subsequently release the chemotherapeutic agent, hence improving the concentration in the brain.[1,2,5,6] These evidences all suggested that glucose could be used as a good carrier for brain targeting drugs. What is more, it is well known that one unique characteristic of cancer cells is that they need more glucose than normal cells, which was known as the Warburg effect. Hence, many malignant cells including the glioma have an overexpression of glucose transporters (GLUTs), especially $GLUT_1$, to maintain their growth and survival. Targeting the Warburg effect as an anticancer strategy has gained a great deal of interest in recent years.[14–16]

Over the past years, our group has done a lot of researches on brain targeting and cancer targeting moieties specially based on glucose or peptides by active process.[17–19] In addition to targeting the Warburg effect to deliver drugs to glioma, RGD sequence, an arginine-glycine-aspartic (Arg-Gly-Asp) tripeptide, has been shown to be another most promising ligand for targeting a range of malignant tumors, including glioma, osteocarcinoma, breast cancer and other human cancers, that are known to overexpress $\alpha_v\beta_3$ receptors.[20,21] Meanwhile, the expression of $\alpha_v\beta_3$ in normal tissue is limited, all of which make it to be an attractive ligand for glioma-targeting.[22] A lot of interesting researches had been done on the nanocarriers modified by RGD.[23–25]

Herein, we aim to construct a dual-targeting moiety Glu-RGD-Chol (Figure 1) as liposomes ligand to delivery PTX not only into brain parenchyma but also into glioma tissue. What's more, the Glu-RGD modified, non-coated, singly modified and co-modified by physical blending liposomes were prepared by the lipid film hydration-ultrasound method, and the characteristics and targeting abilities were conducted *in vitro* and *in vivo*.

2 | RESULTS AND DISCUSSION

2.1 | Chemistry

The synthetic route of ligand Glu-RGD-Chol is illustrated in Scheme 1. Firstly, cholesterol **1**, the starting material, underwent four steps to generate compound **5**,[2] which was then conjugated with diethanol amine in the presence of isobutyl chloroformate (IBCF) and *N*-methyl morpholine (NMM) to give compound **6**. Subsequently, condensation of compound **6** and glucose derivative **14** in the presence of dicyclohexyl carbodiimide (DCC) and 4-dimethylamiopyridine (DMAP) gave **7**, which was then coupled with RGD peptide intermediate **20** to generate **8**. Then, after deprotecting the trimethylsilyl (TMS) groups and the protecting groups of RGD from **8**, the desired conjugate Glu-RGD-Chol was obtained. All the title compounds and important intermedium were characterized by their respective ^{1}H NMR and MS.

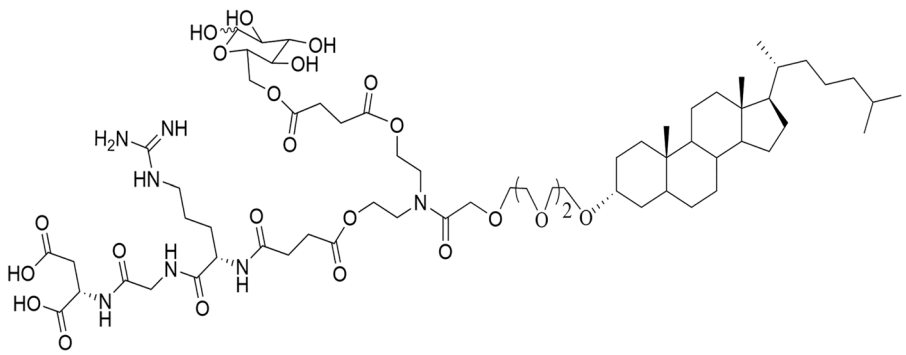

FIGURE 1 The structure of the ligand Glu-RGD-Chol

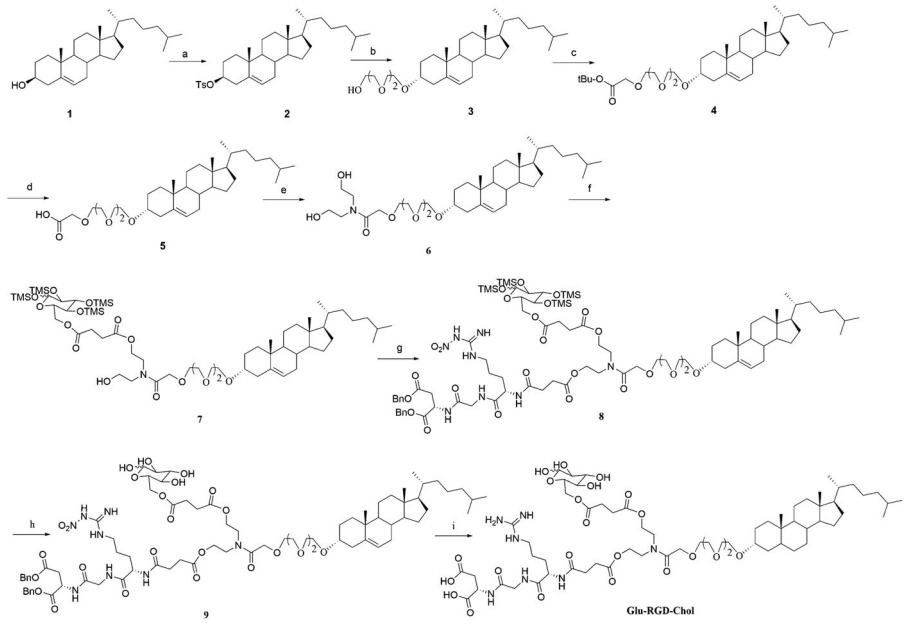

SCHEME 1 Synthesis of ligand Glu-RGD-Chol. Reagents and conditions: (a) TsCl, pyridine, 50°C, 5 h; (b) triethylene glycol, dioxane, reflux, 6 h; (c) *t*-butyl bromoacetate, *n*-$Bu_4N^+HSO_4$, 50% NaOH, toluene, r.t., 16 h; (d) TsOH, tolunene, reflux, 8 h; (e) diethanol amine, IBCF, NMM, CH_2Cl_2, −10°C – r.t., 5 h; (f) **14**, DCC, DMAP, CH_2Cl_2, −5°C – r.t., 5 h; (g) **20**, DCC, DMAP, CH_2Cl_2, −5°C – r.t., 10 h; (h) TFA, CH_2Cl_2, r.t., 3 h; (i) H_2, Pd/C, CH_3OH, 50°C, 24 h

2.2 | Preparation and characterization of liposomes

Proper size and uniform distribution of nanoparticles were required for both BBB permeation and brain tumor targeting. The particle sizes and zeta potentials of different liposomes in this study are listed in Table 1. For the five types of liposomes, encapsulation efficiencies of paclitaxel were all greater than 85%, respectively. The average particle sizes of all liposomes were less than 110 nm, and the values of PDI were less than 0.2, fully complied with the conditions. What's more, the transmission electron microscopy (TEM) of PTX-Glu-RGD-Lip showed that the liposomes exhibited uniform spherical shape (Figure 2). To our knowledge, the particle size and zeta potential of liposomes were crucial to *in vivo* bio-distribution.[26]

2.3 | *In vitro* drug release study

PTX release properties were evaluated in PBS containing 0.1% Tween 80. As shown in Figure 3, free PTX exhibited a rapid release, with over 80% of the drug released into the media within 12 h incubation. On the other hand, PTX-loaded liposomes achieved sustained release behaviors so that the cumulative PTX release of drug-loaded liposomes was less than 60% after 48 h incubation in PBS. No significant difference on release properties was observed among PTX-Lip, PTX-Glu-Lip, PTX-RGD-Lip, PTX-Glu-RGD-Lip and PTX-Glu + RGD-Lip, and none of these PTX-loaded liposomes displayed burst initial release patterns.

2.4 | *In vitro* stability of liposomes in serum

Stability of liposomes under biological conditions is an important parameter governing the activity of the associated therapeutic agent. Transmittance of different liposomes were monitored in the presence of 50% FBS. As shown in Figure 4, the transmittance of the liposomes were above 90% and hardly changed after 48 h incubation with 50% FBS. This stability study of liposomes indicated that the liposomes were enough to prevent the interaction between liposomes and serum protein, which was important to achieve a long blood half-life *in vivo*.

TABLE 1 The composition and characterization of different PTX-loaded liposomes ($n = 3$)

Liposomes	Size (nm)	PDI	Zeta potential (mV)	EE (%)
PTX-Lip	105.8 ± 2.5	0.188 ± 0.023	−2.08 ± 0.12	90.57 ± 3.84
PTX-Glu-Lip	106.3 ± 1.4	0.193 ± 0.009	−3.45 ± 0.29	88.54 ± 5.01
PTX-RGD-Lip	105.1 ± 2.5	0.189 ± 0.010	−3.84 ± 0.34	88.97 ± 3.84
PTX-Glu-RGD-Lip	103.9 ± 3.8	0.192 ± 0.034	−4.56 ± 0.19	85.46 ± 5.69
PTX-Glu + RGD-Lip	107.8 ± 1.9	0.196 ± 0.028	−5.73 ± 0.65	86.94 ± 7.81

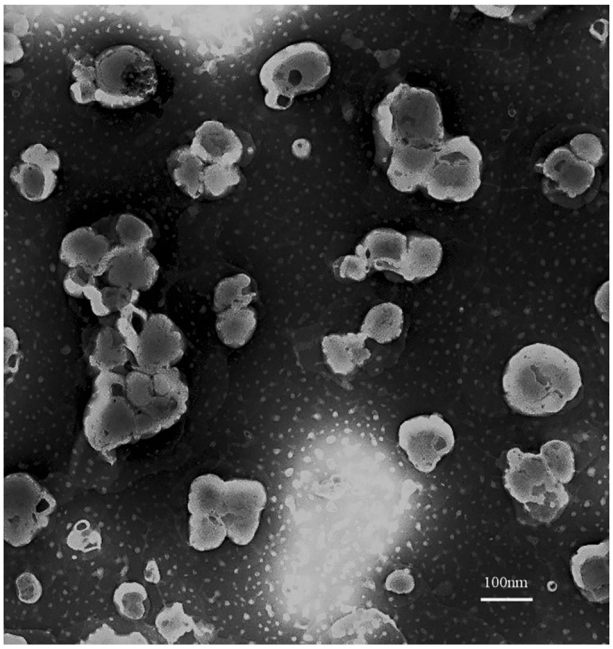

FIGURE 2 The TEM image of PTX-Glu-RGD-Lip

2.5 | Hemolysis assays

Hemocompatibility is a key point for *in vivo* applications of liposomes. As shown in Figure 5, hemolysis assay of ligand-modified liposomes demonstrated that all the liposomes did not show any significant increase in the hemoglobin release up to 400 nmoles of phospholipids. PTX-Glu-RGD-Lip did not display concentration-dependent increase in hemolysis as well and less than 10% hemolysis was always regarded as non-toxic.

2.6 | Cytotoxicity

The cytotoxicity of different liposomes on bEnd.3 cells and C6 cells was evaluated using MTT assay. As shown in Figure 6A and C, free PTX showed higher inhibition rate than PTX-loaded liposomes, because free drugs could be transported into the cells directly without a drug release process. On the other hand, the cytotoxicity of blank liposomes was also measured, and all these five kinds of blank liposomes exhibited no significant cytotoxicity (Figure 6B and D). Therefore, our liposomal drug delivery systems were safe and non-toxic to be further used *in vivo*.

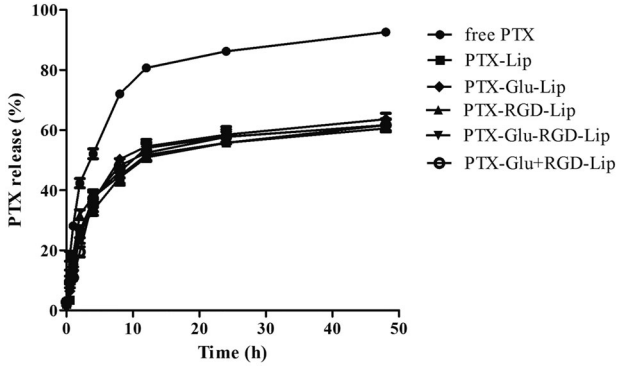

FIGURE 3 The PTX release profiles of free PTX, PTX-Lip, PTX-Glu-Lip, PTX-RGD-Lip, PTX-Glu-RGD-Lip, and PTX-Glu + RGD-Lip in PBS (pH 7.4) containing 0.1% Tween 80 over 48 h (n = 3, mean ± SD)

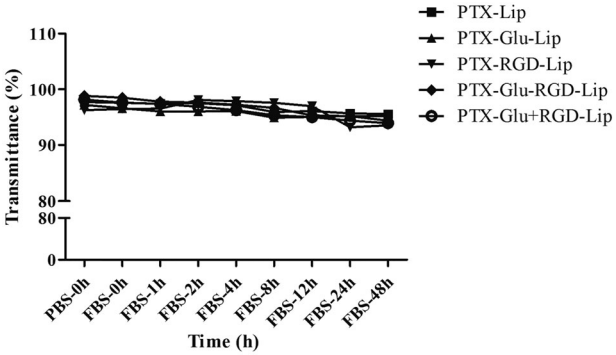

FIGURE 4 The variations of transmittance of different modified liposomes in 50% FBS (n = 3, mean ± SD)

2.7 | Cellular uptake study

The bEnd.3 cells having endothelial properties were widely used as a model for simulating brain capillary endothelial cells and evaluating the BBB penetrating capability *in vitro*. As the transporter $GLUT_1$ and integrin $\alpha_v\beta_3$ receptor were verified to be expressed on both bEnd.3 cells and C6 cells, the cellular uptake of different modified liposomes was studied. Conventional liposomes were used as negative control. Figure 7A depicted that the uptake of Glu-RGD-Lip was 2.42, 1.99, 2.06, and 1.23 times higher than that of Lip, Glu-Lip, RGD-Lip, and Glu + RGD-Lip on bEnd.3 cells, respectively. What's more, Glu-RGD-Lip also showed an excellent uptake on C6 cells, nearly 10-fold higher compared with Lip (Figure 7B). All data showed that Glu-RGD-Lip had better targeting property to $GLUT_1$ and integrin

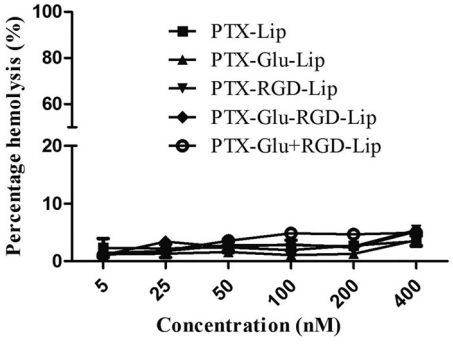

FIGURE 5 Hemolysis percentage of different liposomes. Values are represented as mean ± SD (n = 3)

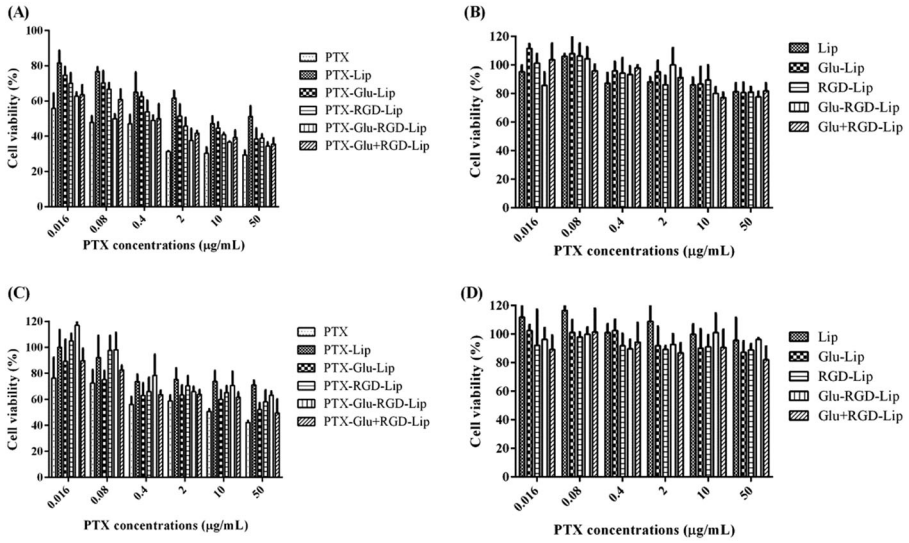

FIGURE 6 (A) The cytotoxicity study of PTX-loaded liposomes and free PTX on C6 cells. (B) The cytotoxicity study of blank liposomes on C6 cells. (C) The cytotoxicity study of PTX-loaded liposomes and free PTX on bEnd.3 cells. (D) The cytotoxicity study of blank liposomes on bEnd.3 cells (mean ± SD, $n = 3$)

$\alpha_v\beta_3$-expressed cells due to the synergistic effect of the dual-mediated endocytosis.

In order to study the uptake mechanism of Glu-RGD-Lip, a series of endocytosis inhibitors were pre-incubated with bEnd.3 cells and C6 cells, and the inhibition rate was calculated to analyze the uptake mechanism. As shown in Figure 7C and D, the preincubation of free glucose or free RGD peptide could competitively inhibit the uptake of Glu-RGD-Lip both on the two cell lines. This further proved that

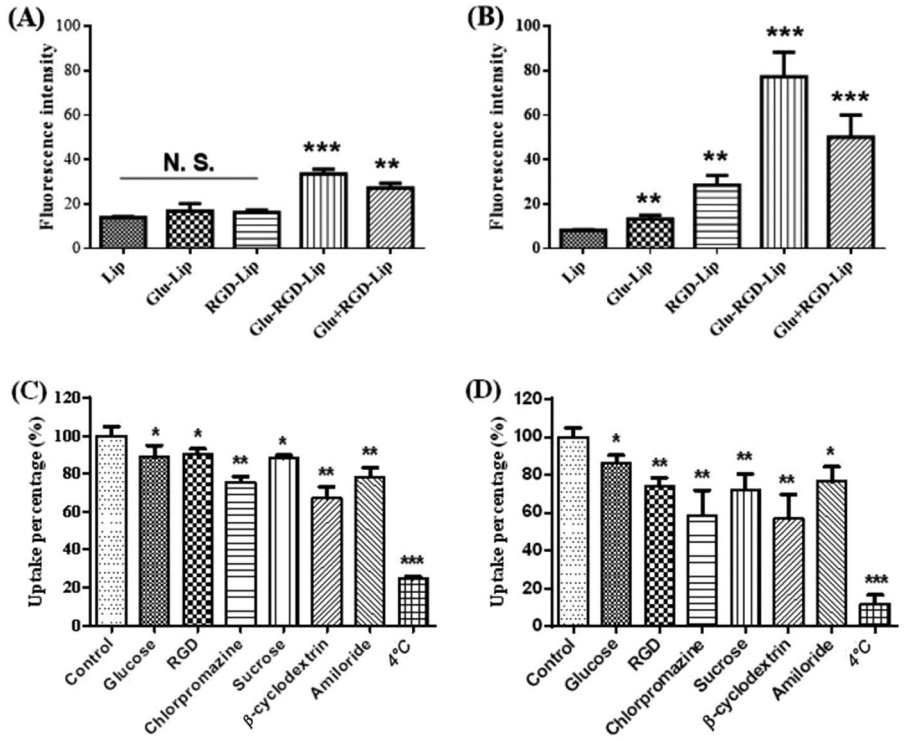

FIGURE 7 Cellular uptake of CFPE-labeled liposomes on bEnd.3 cells (A) and C6 cells (B). Uptake mechanism study of Glu-RGD-Lip on bEnd.3 cells (C) and C6 cells (D) (mean ± SD, $n = 3$), *, **, and *** represent $p < 0.05$, $p < 0.01$, and $p < 0.001$ versus control group, N. S. indicates no significant difference

the glucose domain and RGD domain of liposomes increased the cellular internalization by specifically binding to $GLUT_1$ and $\alpha_v\beta_3$. Furthermore, the effects of clathrin-mediated endocytosis on the internalization of the Glu-RGD-Lip were evaluated using chlorpromazine and sucrose, a kind of clathrin-coated pits formation blocking agent. β-Cyclodextrin, agent disrupting caveolae, was used to evaluate the effect of caveolae-mediated endocytosis on the internalization of the Glu-RGD-Lip. Amiloride was chosen to block micropinocytosis. As the results showed, every inhibitor showed different levels of inhibition effects. 4°C also had a strong effect on cellular uptake (down to 27.74 and 11.84%, respectively), suggesting energy-dependent properties of endocytosis. The images by CLSM (Figure 8) were well consistent with the above results by a flow cytometer. All the results indicated that Glu-RGD-Lip could be recognized by glucose transporter $GLUT_1$ and integrin $\alpha_v\beta_3$ receptor on the outer membrane of cells via the residues on the surface, and then energy-dependently internalized through a synthetic endocytic pathway including clathrin-mediated, caveolae-mediated and micropinocytosis-mediated endocytosis.

2.8 | Distribution in brain and pharmacokinetic studies in mice

For *in vivo* study, PTX-Lip, PTX-Glu-Lip, PTX-RGD-Lip, PTX-Glu-RGD-Lip, PTX-Glu + RGD-Lip and paclitaxel original drug were injected through caudal vein of the mice with a single dose equivalent to 10 mg/kg body weight of paclitaxel. At 5, 15, 30, 60, 120, 240, 480, and 1440 min after injection, blood sample was collected from the eye socket of mice, and placed in tubes containing heparin. Then blood and brain were collected to analyze the concentration of paclitaxel at different intervals by HPLC method.

The plasma PTX concentration-time profiles are shown in Figure 9 and the pharmacokinetic parameters of PTX from different formulations are summarized in Table 2. The results showed that the area under the concentration-time profile (AUC_{0-t}) of paclitaxel in the five types of liposomes was much higher than that of naked paclitaxel within 24 h. The (AUC_{0-t}) was increased by about 1.83-time for PTX-Glu-RGD-Lip compared to free PTX. In addition, it was also shown that PTX-Glu-RGD-Lip could extend the elimination half-life ($t_{1/2}$) of free PTX from 235 to 561 min. These data indicated that the liposomes showed certain stability which would increase the chance to be transported across BBB.

To further evaluate the possibility of the Glu-RGD-mediated liposomes being transported across BBB, the distribution in brain of PTX-loaded liposomes and paclitaxel was determined. The concentrations of paclitaxel in brain versus time curves are displayed in Figure 10 and the pharmacokinetic parameters are listed in Table 3.

In brain, it is obvious that all of the liposomes could be delivered to the brain following i.v. administration. At different time interval, the concentration of paclitaxel released from liposomes was much higher than that from paclitaxel original drug during 24 h. The AUC_{0-t} and C_{max} of paclitaxel in brain after i.v. administration of liposomes were fairly higher than that after the injection of free paclitaxel. The relative uptake efficiencies (REs) were enhanced to 1.26, 3.80, 1.73, 4.41, and 4.06 times than that of naked paclitaxel for liposomes PTX-Lip, PTX-Glu-Lip, PTX-RGD-Lip, PTX-Glu-RGD-Lip, and PTX-Glu + RGD-Lip, respectively. The concentration efficiencies (CEs) were also enhanced to 1.03, 3.85, 2.44, 4.72, and 4.61 times than that of paclitaxel. So these data further proved our conjecture that liposome with ligand Glu-RGD can deliver and keep paclitaxel in the CNS.

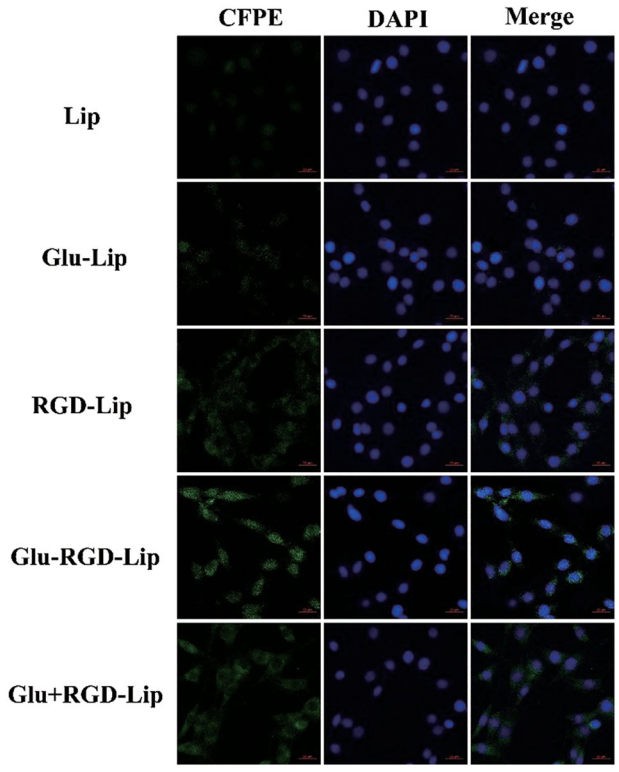

FIGURE 8 Qualitative cellular uptake of CFPE-labeled liposomes on C6 cells

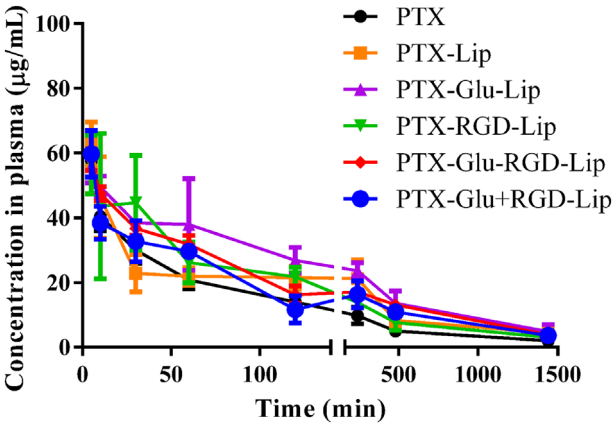

FIGURE 9 The concentration curve of paclitaxel versus time in plasma after i.v. injection of paclitaxel and PTX-loaded liposomes in mice ($n = 5$)

TABLE 2 Pharmacokinetic parameters of paclitaxel in blood after administration of paclitaxel and liposomes (n = 5)

	Paclitaxel	PTX-Lip	PTX-Glu-Lip	PTX-RGD-Lip	PTX-Glu-RGD-Lip	PTX-Glu + RGD-Lip
$AUC_{(0-t)}$ (μg/mL · min)	9617.65 ± 2062.56	15495.21 ± 2124.35	20914.38 ± 2843.02	13756.15 ± 2008.70	17648.27 ± 1098.55	15338.97 ± 1735.69
MRT (min)	359.99 ± 37.98	427.04 ±73.06	413.40 ± 51.05	376.30 ± 89.21	423.13 ± 15.74	425.41 ± 60.51
T_{max} (min)	5	6	6	6	5	5
C_{max} (μg/mL)	57.60 ± 6.87	65.45 ± 4.44	56.85 ± 4.54	64.81 ± 10.28	57.98 ± 3.39	59.77 ± 7.20
$t_{1/2}$ (min)	235.24 ± 44.79	441.10 ± 197.25	498.99 ± 96.79	370.70 ± 207.57	561.23 ± 100.38	486.76 ± 130.69

2.9 | *In vivo* imaging

Kunming mice bearing C6 glioma were used to estimate the glioma targeting efficiency of different liposomes. Figure 11 shows the *in vivo* images of intracranial C6 glioma bearing mice at different time points after systemic administration of DiD-loaded liposomes. For RGD-Lip group, the trace fluorescence in brain region indicated that modification of RGD peptide had limited increase for liposomes to penetrate across the BBB. It was perspicuously observed that the fluorescence signal of Glu-RGD-Lip in the brain was stronger than other groups from 1 to 24 h after systemic administration, displaying the strongest glioma targeting capability of Glu-RGD-Lip. All of the results suggested that Glu-RGD on the surface of liposomes endowed the liposomes with brain glioma dual-targeted delivery capability: Firstly this delivery system traversed the BBB via the recognition of the facilitative $GLUT_1$ on the BBB, and then was internalized by the glioma cells via $GLUT_1$ and $\alpha_v\beta_3$ mediated endocytosis. These findings were well consistent with the results of *in vitro* cellular uptake study.

3 | CONCLUSION

In order to develop an efficient glioma targeting drug delivery system to greatly improve the ability to target glioma, a novel dual-targeting glucose-RGD derivative was designed and synthesized as liposome ligand in this work. Glu-RGD-Lip could be recognized by glucose transporter $GLUT_1$ and integrin $\alpha_v\beta_3$ receptor on the outer membrane of cells via the residues on the surface, and then energy-dependently internalized through a synthetic endocytic pathway including clathrin-mediated, caveolae-mediated, and micropinocytosis-mediated endocytosis. What is more, Glu-RGD-Lip was proved to increase the transport of the liposomes across the BBB through $GLUT_1$-mediated transcytosis and afterwards target the brain glioma through $GLUT_1$ and $\alpha_v\beta_3$ *in vivo*. Therefore, the Glu-RGD modification represents a promising strategy for the development of future brain-specific drug delivery systems.

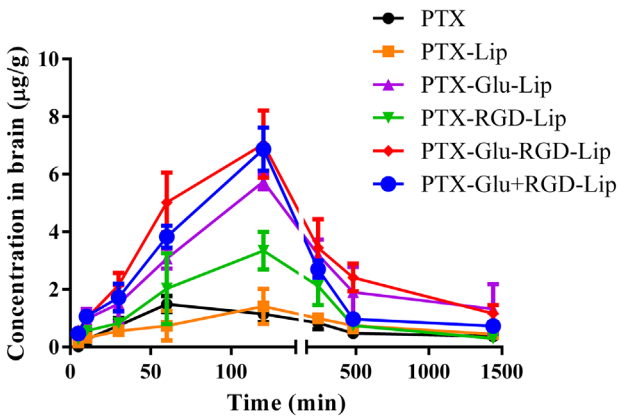

FIGURE 10 The concentration curve of paclitaxel versus time in brain after i.v. injection of paclitaxel and PTX-loaded liposomes in mice (n = 5)

4 | EXPERIMENTAL

4.1 | General

All liquid reagents were distilled before use. All unspecified reagents were from commercial resources. TLC was performed using precoated silica gel GF254 (0.2 mm), while column chromatography was performed using silica gel (100–200 mesh). The melting point was measured on a YRT-3 melting point apparatus (Shantou Keyi instrument & Equipment Co. Ltd, Shantou, China). Elemental analyses were performed by Atlantic Microlab (Atlanta, GA, USA). ^{1}H NMR spectra were taken on a Varian INOVA 400/600 (Varian, Palo Alto, CA, USA) using $CDCl_3$, d_6-DMSO and CD_3OD as solvent. Chemical shifts are expressed in δ (ppm), with tetramethylsilane (TMS) functioning as the internal reference, and coupling constants (J) were expressed in Hz. Mass spectra were recorded on an Agilent 1946B ESI-MS instrument (Agilent, Palo Alto, CA, USA). Paclitaxel and docetaxel were obtained from National Institute for Food and Drug Control. Soybean phospholipids (SPC) were purchased from Kelong Chemical. Cholesterol (Chol) was purchased from Bio Life Science & Technology Co., Ltd. (Shanghai, People's Republic of China). A Diamonsil column (200 × 4.6 mm, 5 mm) was used. A LC-10A liquid chromatographic system (Shimadzu) and a reverse-phase HPLC column (ODS-C18 column, 4.6 × 200 mm, 5 μm, SinoChrom, Dalian, P.R. China) were used.

The InChI codes of the inverstigated compounds are provided as Supporting Information.

TABLE 3 Pharmacokinetic parameters of paclitaxel in brain after administration of paclitaxel and liposomes (n = 5)

	Paclitaxel	PTX-Lip	PTX-Glu-Lip	PTX-RGD-Lip	PTX-Glu-RGD-Lip	PTX-Glu + RGD-Lip
$AUC_{(0-t)}$ (μg/g · min)	805.85 ± 181.60	1018.84 ± 149.47	3062.68 ± 943.86	1393.83 ± 87.38	3555.90 ± 686.12	3272.55 ± 259.40
MRT (min)	548.37 ± 42.52	566.21 ± 71.85	527.49 ± 86.72	396.63 ± 19.90	489.08 ± 29.79	432.68 ± 29.24
T_{max} (min)	60	144	120	132	120	120
C_{max} (μg/g)	1.49 ± 0.27	1.54 ± 0.46	5.74 ± 0.26	3.64 ± 0.49	7.04 ± 1.17	6.87 ± 0.74
$t_{1/2}$ (min)	310.26 ± 138.69	598.10 ± 315.68	718.03 ± 204.11	543.76 ± 251.15	847.43 ± 230.10	526.11 ± 198.60
Re	–	1.26	3.80	1.73	4.41	4.06
Ce	–	1.03	3.85	2.44	4.72	4.61

4.2 | Chemistry

4.2.1 | Synthesis of compounds 2–5

The synthesis of compounds **2–5** was reported in our previous work.[2]

4.2.2 | Synthesis of compound 6

To a solution of compound **5** (4.00 g, 6.93 mmol) in CH_2Cl_2 (25 mL) was added NMM (0.84 mL, 7.63 mmol) and IBCF (0.96 mL, 7.63 mmol), and the reaction was stirred at −10°C for 15 min. Then diethanol amine (1.09 g, 10.40 mmol) in CH_2Cl_2 (5 mL) was added slowly. After stirring for another 5 h at r.t., the mixture was washed with 1 mol/L HCl, saturated $NaHCO_3$ and saturated NaCl. The organic layer was dried over anhydrous Na_2SO_4, and concentrated *in vacuo*. The residue was purified by flash column chromatography to afford **6** (4.09 g, 89%) as a yellow oil. ^{1}H NMR (400 MHz, $CDCl_3$, ppm) δ: 0.67 (s, 3H), 0.86 (d, 6H, J = 6.4 Hz), 0.91 (d, 3H, J = 6.4 Hz), 0.99 (s, 3H), 1.01–2.38 (remaining cholesterol protons), 3.14–3.21 (m, 1H), 3.50–3.85 (m, 20H), 4.28 (s, 2H), 5.34 (d, 1H, J = 4.8 Hz).

4.2.3 | Synthesis of compound 7

To a solution of compound **14** (0.15 g, 0.26 mmol) in 15 mL dichloromethane was added DCC (63 mg, 0.31 mmol) and cat. DMAP, then the mixture was stirred at −5°C for 30 min. Compound **6** (0.17 g, 0.26 mmol) in CH_2Cl_2 (5 mL) was added to the above reaction mixture promptly. After stirring for 5 h at room temperature, the reaction was terminated and then filtered. The filtrate was concentrated, and the residue was purified by flash chromatography to yield **7** (0.15 g, 59%) as a yellow oil. ^{1}H NMR (400 MHz, $CDCl_3$, ppm) δ: 0.18 (s, 36H), 0.73 (s, 3H), 0.88 (d, 6H, J = 6.4 Hz), 0.96 (d, 3H, J = 6.4 Hz), 1.03 (s, 3H), 0.73–2.38 (remaining cholesterol protons), 2.62–2.67 (m, 4H), 2.86 (s, 2H), 3.14–3.19 (m, 1H), 3.41–3.89 (m, 21H), 3.99–4.03 (m, 1H), 4.20–4.31 (m, 4H), 4.38 (d, 1H, J = 11.6 Hz), 5.03 (s, 1H), 5.35 (s, 1H).

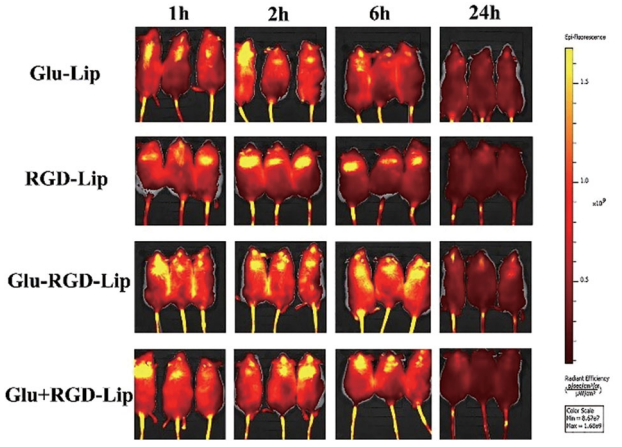

FIGURE 11 *In vivo* images of intracranial C6 glioma bearing mice at different time points after systemic administration of DiD-loaded liposomes

4.2.4 | Synthesis of compound 8

To a solution of compound **20** (44 mg, 0.066 mmol) in 5 mL dichloromethane was added DCC (16 mg, 0.079 mmol) and cat. DMAP, then the mixture was stirred at −5°C for 30 min. Compound **7** (80 mg, 0.066 mmol) in CH_2Cl_2 (3 mL) was added to the above reaction mixture slowly. After stirring for 10 h at room temperature, the reaction was terminated and then filtered. The filtrate was concentrated, and the residue was purified by flash chromatography to give **8** (40 mg, 33%) as a yellow oil. ^{1}H NMR (400 MHz, $CDCl_3$, ppm) δ: 0.13 (s, 36H), 0.66 (s, 3H), 0.86 (d, 6H, J = 6.4 Hz), 0.91 (d, 3H, J = 6.4 Hz), 0.97 (s, 3H), 1.00–2.35 (remaining cholesterol protons), 2.48–2.68 (m, 8H), 2.90–2.98 (s, 2H), 3.18–3.19 (m, 1H), 3.34–4.43 (m, 31H), 4.89 (s, 1H), 5.00 (d, 1H, J = 2.4 Hz), 5.05 (s, 2H), 5.10 (s, 2H), 5.33 (s, 1H), 7.28–7.32 (m, 10H), 7.46–7.78 (m, 4H).

4.2.5 | Synthesis of compound 9

To a solution of compound **8** (50 mg, 0.027 mmol) in CH_2Cl_2 (8 mL) was added trifluoracetic acid (2.0 mL) at 0°C and then the reaction was stirred for 3 h at room temperature. The mixture was concentrated and the residue was purified by chromatography to give compound **9** (25 mg, 59%) as a colorless oil. ^{1}H NMR (600 MHz, CD_3OD, ppm) δ: 0.70 (s, 3H), 1.00 (s, 3H), 0.70–2.37 (remaining cholesterol protons), 2.51–2.62 (m, 10H), 3.62–3.67 (m, 20H), 3.83–3.93 (m, 3H), 4.19–4.33 (m, 9H), 5.08–5.12 (m, 4H), 5.32–5.34 (m, 2H), 7.32 (s, 10H).

4.2.6 | Synthesis of ligand Glu-RGD-Chol

To a solution of compound **9** (50 mg, 0.019 mmol) in CH_3OH (6 mL), Pd/C (10 mg, 10%) was added. Then, the mixture was stirred in

hydrogen atmosphere at 50°C for 24 h. Pd/C was filtered and the filtrate was concentrated to give ligand Glu-RGD-Chol (20 mg, 78%) as a white solid. ^{1}H NMR (400 MHz, CD_3OD, ppm) δ: 0.65 (s, 3H), 0.83–2.50 (remaining cholesterol protons), 2.57–2.64 (m, 10H), 2.81 (s, 3H), 2.87–3.22 (m, 5H), 3.33–3.36 (m, 2H), 3.54–3.66 (m, 27H), 3.76–3.97 (m, 4H), 4.16–4.36 (m, 14H), 4.47–4.50 (m, 1H), 4.62 (br, 1H), 5.08 (d, 2H, J = 3.6 Hz). ESI-MS calculated for $C_{65}H_{108}N_7O_{23}$ $[M-H]^-$ 1354.7, found: 1354.4.

4.2.7 | Synthesis of glucose derivatives, RGD peptide intermediates, ligand Glu-Chol and RGD-Chol

The detailed synthetic procedures of glucose derivatives, RGD peptide intermediates, ligand Glu-Chol and RGD-Chol are given in the Supporting Information.

4.3 | Preparation and characterization of liposomes

Liposomes were prepared by thin film hydration method. Lipid compositions of the prepared liposomes were as follows: (1) conventional liposomes (Lip), SPC/cholesterol (molar ratio = 62:33); (2) ligand Glu-RGD-Chol modified liposomes (Glu-RGD-Lip), SPC/cholesterol/ligand Glu-RGD-Chol (molar ratio = 62:33:3); (3) ligand Glu-Chol modified liposomes (Glu-Lip), SPC/cholesterol/ligand Glu-Chol (molar ratio = 62:33:3); (4) ligand RGD-Chol modified liposomes (RGD-Lip), SPC/cholesterol/ligand RGD-Chol (molar ratio = 62:33:3); (5) ligand Glu-Chol and RGD-Chol co-modified liposomes (Glu + RGD-Lip), SPC/cholesterol/ligand Glu-Chol/RGD-Chol (molar ratio = 62:33:3:3). All lipid materials were dissolved in the mixture solvent chloroform/methanol (v/v = 2:1), and then the organic solvent was removed by rotary evaporation to form a lipid film. After kept in vacuum overnight, the obtained film was hydrated in PBS (pH 7.4) for 0.5 h at 20°C. Then it was further intermittently sonicated by a probe sonicator at 80 W for 80 s to form liposomes. PTX-loaded liposomes were prepared with paclitaxel added to the lipid organic solution prior to the solvent evaporation. The entrapment efficiency of paclitaxel was determined by HPLC. Likewise, CFPE-labeled liposomes were prepared by adding appropriate amount of CFPE to the solution before the solvent evaporation. The mean size and zeta potential of Lip, Glu-RGD-Lip, Glu-Lip, RGD-Lip and Glu + RGD-Lip were detected by Malvern Zeta sizer Nano ZS90 (Malvern Instruments Ltd., UK).

4.4 | *In vitro* drug release study

In vitro paclitaxel release study was performed using dialysis method. Each PTX-loaded liposomes (0.4 mL) or free paclitaxel were placed into dialysis tubes (MWCO = 8000–14000 Da) and tightly sealed. Then the dialysis tubes were placed into 40 mL PBS containing 0.1% (v/v) Tween 80 and incubated under 37°C for 48 h with gentle oscillating at 45 rpm. At predetermined time points (0, 1, 2, 4, 8, 12, 24, and 48 h), 0.1 mL release medium was taken out and replaced with equal volume of fresh release medium. Then the samples were diluted with acetonitrile and the concentrations of paclitaxel were determined at the wavelength of 225 nm by HPLC.

4.5 | *In vitro* stability of liposomes in serum

Turbidity variations were measured to demonstrate the serum stability of liposomes in the presence of fetal bovine serum (FBS). Briefly, liposomes were mixed with equal volume of FBS under 37°C with moderate shaking at 45 rpm. The transmittance of the mixture was measured at predetermined time points (0, 1, 2, 4, 8, 12, 24, and 48 h) at 750 nm by a microplate reader (Thermo Scientific Varioskan Flash, USA).

4.6 | Hemolysis assays

To evaluate the safety of ligands-modified liposomes during body circulation, hemolysis assay was performed. Fresh mouse blood was collected in tubes containing heparin sodium. The red blood cells (RBCs) were separated and collected by centrifugation at 5×10^3 rpm for 5 min and washed several times with PBS until the supernatant became colorless. After the last wash, the RBCs were diluted with PBS to a concentration of 2% (v/v). Various concentrations of liposomes were incubated with equal volume of 2% RBCs solutions for 1 h at 37°C with gentle shaking, followed by centrifugation at 1×10^4 rpm for 10 min. Absorbance of hemoglobin was measured using a microplate reader (Thermo Scientific Varioskan Flash) at 540 nm. The values for 0% and 100% hemolysis were determined by incubating erythrocytes with PBS or 1% (v/v) Triton X-100. The hemolysis percentage was calculated using the following equation:

$$\text{The percent hemolysis} = \left(A_{\text{Sample}} - A_{\text{Negative}}\right) / \left(A_{\text{Positive}} - A_{\text{Negative}}\right) \times 100\%$$

where A is the ultraviolet absorbance of hemoglobin.

4.7 | Cytotoxicity

Murine brain endothelial cells (bEnd.3) and glioma cells (C6) were cultured in Dulbecco's modified Eagle medium (DMEM) supplemented with 10% fetal bovine serum (FBS), 100 U/mL streptomycin and 100 U/mL penicillin at 37°C in a 5% CO_2 humidified environment incubator (Thermo Scientific, USA).

The cytotoxicity of PTX-loaded liposomes was measured with MTT assay. Generally, the cells were seeded in a 96-well plate at a density of 5×10^3 cells/well and cultured for 24 h at 37°C. PTX-loaded liposomes and free paclitaxel were diluted to predetermined concentrations with PBS, and added into each well for 24 h incubation. The final concentrations of paclitaxel were in the range of 0.016–50 μg/mL. Blank liposomes were added at the same concentration of PTX-loaded liposomes. Then, 20 μL MTT solutions (5.0 mg/mL) was added to the medium and incubated for another 4 h at 37°C. After removal of the culture medium, the

reduced MTT dye was solubilized by DMSO (150 µL) and the absorbance was read at 490 nm wavelength on an automatic microplate spectrophotometer. Cell viability (%) was calculated as the following equation: $A_{test}/A_{control} \times 100\%$, where A_{test} and $A_{control}$ represented the absorbance of treated cells and control cells, respectively.

4.8 | Cellular uptake study

4.8.1 | Cellular uptake

bEnd.3 cells and C6 cells were seeded in 6-well plates at a density of 5×10^5 cells/well and cultured for 24 h at 37°C. Different liposomes were added into each well with a final concentration of CFPE at 2 µg/mL. After cultured for 4 h at 37°C, trypsin was used to harvest the cells, which were washed three times with PBS afterward, and finally resuspended in 0.5 mL PBS. Then, the fluorescent intensity of cells treated with different liposomes was measured by a flow cytometer (Cytomics FC 500, Beckman Coulter, USA).

For confocal microscope studies, C6 cells were plated onto a 6-well plate containing cover glass at a density of 5×10^5 cells/well and cultured for 24 h at 37°C. CFPE-labeled liposomes were added into each well and allowed for further co-incubation for 4 h. Following that, the cells were rinsed with cold PBS three times and fixed with 4% paraformaldehyde for 30 min at room temperature, and then cell nuclei were stained with DAPI (1 µg/mL) for 5 min. Finally, the samples were imaged using laser scanning confocal microscope (CLSM) (TCS SP5 AOBS confocal microscopy system, Leica, Germany).

4.8.2 | Uptake mechanism study

In order to study the uptake mechanism of Glu-RGD-Lip, bEnd.3 cells and C6 cells were preincubated with various endocytosis inhibitors, such as chlorpromazine (20 µg/mL), sucrose (137 mg/mL), β-cyclodextrin (5.68 mg/mL), and amiloride (1.48 mg/mL).[27–29] What is more, the inhibition of free glucose (5 mg/mL) and free RGD peptide (0.2 mg/mL), and the effect of temperature were also performed. Briefly, the cells were preincubated with different inhibitors for 30 min at 37°C, then the inhibitors were withdrawn from the wells and CFPE-labeled Glu-RGD-Lip was added. After cultured for 4 h at 37°C, the cells were treated as described in 4.8.1 and the fluorescent intensity was measured by a flow cytometer.

4.9 | Distribution in brain and pharmacokinetic studies in mice

4.9.1 | HPLC analysis of liposomes

The naked paclitaxel and paclitaxel encapsulated liposomes (PTX-Lip, PTX-Glu-Lip, PTX-RGD-Lip, PTX-Glu-RGD-Lip, PTX-Glu + RGD-Lip) were measured by LC-10A liquid chromatographic system (Shimadzu). The analytical column was a reverse-phase HPLC column (ODS-C18 column, 4.6 × 200 mm, 5 µm, SinoChrom) maintaining at 30°C. The mobile phase consisted of water/methanol (67:33) with a low flow rate 1.0 mL/min. The sample volume injected was 20 µL and the detection wavelength was 227 nm.

4.9.2 | Test animals

Adult Kunming mice weighing 20–22 g were obtained from the animal center of Sichuan University. The animals were left for 2 days to acclimatize to animal room conditions and were maintained on standard pellet diet and water *ad libitum*. Food was withdrawn on the day before the experiment, but free access to water was allowed. Since the experiment could be completed within 24 h, there was no significant change in the mice's body weight during the experiment. All animals received human care, and the study protocols complied with the guidelines of Sichuan University animal ethical experimentation committee. Throughout the experiments, the animals were handled according to the requirements of the National Act on the use of experimental animals (People's Republic of China).

4.9.3 | Sample preparation

Blood was collected from the eye socket of mouse into a tube containing heparin sodium, and centrifuged at 5000 rpm for 5 min. The supernatant was collected as plasma sample. The animals were killed by cervical dislocation, and the brains were removed and flushed with saline for three times to remove the remaining blood and then the brains were rolled over on the filter paper carefully to remove the main vessel. All the tissues were homogenized with triple amount of saline. An aliquot of 10 µL of internal standard (docetaxel, 30 µL, 100 µg/mL) was added into 100 µL plasma or 100 µL brain homogenate, and extracted with 200 µL ether. The mixture was vortexed for 5 min, and centrifuged at 10000 rpm for 10 min. The supernatant was transferred to another centrifuge tube, and dried under air stream at room temperature. The dry residue was reconstituted with 100 µL of methanol. The solution was centrifuged at 10000 rpm for 10 min, and then 20 µL of the supernatant was injected into the HPLC system for analysis.

4.9.4 | Body distribution study

Kunming mice were randomly divided into groups for each liposome or paclitaxel. PTX-Lip, PTX-Glu-Lip, PTX-RGD-Lip, PTX-Glu-RGD-Lip, PTX-Glu + RGD-Lip and paclitaxel were given to the mice via the tail vein and each was equivalent to the administration dose of paclitaxel of 10 mg/kg. At 5, 15, 30, 60, 120, 240, 480, and 1440 min after injection, blood samples were collected from the eye socket of mice and placed in tubes containing heparin sodium. After exsanguinations, the mice were killed by cervical dislocation and the brain was removed and washed twice with saline. The brain was weighed and prepared as described earlier. The concentration of paclitaxel was analyzed by HPLC.

4.9.5 | Statistical analysis

The area under the concentration-time profile (AUC_{0-t}), maximal concentration (C_{max}), and mean residence times (MRT) were calculated

by Data and max Statistics (DAS 2.0, Shanghai, China). Statistical evaluation was performed using analysis of variance followed by *t*-test. A value of $p < 0.05$ was considered significant. The relative uptake efficiency (RE) and concentration efficiency (CE) were calculated to evaluate the brain targeting property of liposome. The value of RE and CE were defined as follows:

$$RE = (AUC_{0-t})_L/(AUC_{0-t})_P$$

$$CE = (C_{max})_L/(C_{max})_P,$$

where L and P represented the liposomes loading PTX and paclitaxel, respectively.

4.10 | *In vivo* imaging

Kunming mice were anesthetized with 5% chloral hydrate and placed on a stereotaxic apparatus. C6 cells (2×10^8 cells/mL) were injected into the striatum (1.8 mm lateral, 0.6 mm anterior to the bregma and 3 mm of depth) of each mouse. After 10 days, the mice were randomly divided into four groups (three in each group) and were intravenously injected via the caudal vein of the tumor-bearing mice with DiD-Glu-Lip, DiD-RGD-Lip, DiD-Glu-RGD-Lip, and DiD-Glu + RGD-Lip. Then, the mice were imaged with IVI Spectrum system (Caliper, Hopkington, MA, USA) at 1, 2, 6, and 24 h after injection.

ACKNOWLEDGMENTS

This work was supported by the National Natural Science Foundation of China (Nos. 81573286, 81773577, and 21472130) and the Sichuan Science and Technology Program (2018JY0537), the Fundamental Research Funds for the Central Universities (2012017yjsy211).

CONFLICT OF INTEREST

The authors declare no competing financial interest

ORCID

Yong Wu http://orcid.org/0000-0003-0719-4963

REFERENCES

[1] X. C. Li, B. Y. Qu, X. X. Jin, L. Hai, Y. Wu, *J. Drug Target*. **2014**, *22*, 251.
[2] B. Y. Qu, X. C. Li, M. Guan, X. Li, L. Hai, Y. Wu, *Eur. J. Med. Chem*. **2014**, *72*, 110.
[3] W. Fan, Y. Wu, X. K. Li, N. Yao, X. Li, Y. G. Yu, L. Hai, *Eur. J. Med. Chem*. **2011**, *46*, 3651.
[4] Y. Zhao, B. Y. Qu, X. Y. Wu, X. C. Li, Q. Q. Liu, X. X. Jin, L. Guo, L. Hai, Y. Wu, *Eur. J. Med. Chem*. **2014**, *82*, 314.
[5] B. Y. Qu, X. Li, J. B. Wu, X. L. Li, L. Hai, Y. Wu, *Lett. Org. Chem*. **2012**, *9*, 390.
[6] F. L. Xie, N. Yao, Y. Qin, Q. Y. Zhang, H. L. Chen, M. Q. Yuan, J. Tang, X. K. Li, W. Fan, Q. Zhang, Y. Wu, L. Hai, Q. He, *Int. J. Nanomed*. **2012**, *7*, 163.
[7] H. L. Gao, *J. Neuroimmune Pharm*. **2017**, *12*, 6.
[8] H. L. Gao, Y. Xiong, S. Zhang, Z. Yang, S. J. Cao, X. G. Jiang, *Mol. Pharmaceut*. **2014**, *11*, 1042.
[9] Y. Y. Liu, R. Ran, J. T. Chen, Q. F. Kuang, J. Tang, L. Mei, Q. Y. Zhang, H. L. Gao, Z. R. Zhang, Q. He, *Biomaterials* **2014**, *35*, 4835.
[10] S. B. Ruan, L. Qin, W. Xiao, C. Hu, Y. Zhou, R. R. Wang, X. Sun, W. Q. Yu, Q. He, H. L. Gao, *Adv. Funct. Mater*. **2018**, *28*, 1802227.
[11] H. L. Gao, *Acta Pharm. Sin. B*. **2016**, *6*, 268.
[12] Y. Zhao, L. Zhang, Y. Peng, Q. M. Yue, L. Hai, L. Guo, Q. T. Wang, Y. Wu, *Chem. Biol. Drug Des*. **2018**, *91*, 707.
[13] Q. Chen, T. Gong, J. Liu, X. L. Wang, H. L. Fu, Z. R. Zhang, *J. Drug Target*. **2009**, *17*, 318.
[14] Q. L. He, I. Minn, Q. L. Wang, P. Xu, S. A. Head, E. Datan, B. Yu, M. G. Pomper, J. O. Liu, *Angew. Chem*. **2016**, *55*, 12035.
[15] M. Patra, S. G. Awuah, S. J. Lippard, *J. Am. Chem. Soc*. **2016**, *138*, 12541.
[16] M. Patra, T. C. Johnstone, K. Suntharalingam, S. J. Lippard, *Angew. Chem*. **2016**, *55*, 2550.
[17] Q. M. Yue, Y. Peng, Y. Zhao, R. X. Lu, Q. Y. Fu, Y. Chen, Y. Yang, L. Hai, L. Guo, Y. Wu, *Drug Deliv*. **2018**, *25*, 426.
[18] B. Jiang, J. H. Cao, J. Zhao, D. S. He, J. Z. Pan, Y. H. Li, L. Guo, *Drug Deliv*. **2012**, *19*, 317.
[19] Y. Zhao, D. S. He, L. F. Ma, L. Guo, *Lett. Drug Des. Discov*. **2015**, *12*, 585.
[20] Y. B. Zhao, D. Y. Lin, F. B. Wu, L. Guo, G. He, L. Ouyang, X. R. Song, W. Huang, X. Li, *Int. J. Mol. Sci*. **2014**, *15*, 17565.
[21] B. Jiang, J. Zhao, Y. H. Li, D. S. He, J. Z. Pan, J. H. Cao, L. Guo, *Lett. Org. Chem*. **2013**, *10*, 594.
[22] C. X. Zhang, W. Y. Zhao, L. Liu, R. J. Ju, L. M. Mu, Y. Zhao, F. Zeng, H. J. Xie, Y. Yan, W. L. Lu, *Oncotarget* **2015**, *6*, 32681.
[23] W. Xiao, J. Y. Xiong, S. Zhang, Y. Xiong, H. J. Zhang, H. L. Gao, *Int. J. Pharmaceut*. **2018**, *538*, 105.
[24] S. B. Ruan, Q. He, H. L. Gao, *Nanoscale* **2015**, *7*, 9487.
[25] S. B. Ruan, W. Xiao, C. Hu, H. J. Zhang, J. D. Rao, S. H. Wang, X. Wang, Q. He, H. L. Gao, *Acs Appl. Mater. Inter*. **2017**, *9*, 20348.
[26] L. H. Wang, Y. Zhao, R. X. Lu, Y. Peng, L. Guo, L. Hai, M. Guan, Y. Wu, *NANO* **2018**, *13*, 1850008.
[27] W. W. Du, Y. C. Fan, N. Zheng, B. He, L. Yuan, H. Zhang, X. Q. Wang, J. C. Wang, X. Zhang, Q. Zhang, *Biomaterials* **2013**, *34*, 794.
[28] B. Nichols, *J. Cell Sci*. **2003**, *116*, 4707.
[29] X. Y. Jiang, H. L. Xin, Q. Y. Ren, J. J. Gu, L. J. Zhu, F. Y. Du, C. L. Feng, Y. K. Xie, X. Y. Sha, X. L. Fang, *Biomaterials* **2014**, *35*, 518.

SUPPORTING INFORMATION

Additional supporting information may be found online in the Supporting Information section at the end of the article.

How to cite this article: Fu Q, Zhao Y, Yang Z, et al. Liposomes actively recognizing the glucose transporter $GLUT_1$ and integrin $\alpha_v\beta_3$ for dual-targeting of glioma. *Arch Pharm Chem Life Sci*. 2019;1–11. https://doi.org/10.1002/ardp.201800219